Presence of Two Freezing-In Processes Concerning α-Glass Transition in the New Liquid Phase of Triphenyl Phosphite and Its Consistency with "Cluster Structure" and "Intracluster Rearrangement for α Process" Models

Mayumi Mizukami, Kazuhisa Kobashi,† Minoru Hanaya, and Masaharu Oguni*

Department of Chemistry, Faculty of Science, Tokyo Institute of Technology, Ookayama-2, Meguro-ku, Tokyo 152-8551, Japan

Received: September 29, 1998; In Final Form: February 2, 1999

Triphenyl phosphite was studied by powder X-ray diffractometry, adiabatic calorimetry, and dielectric relaxation measurements. The highly correlated liquid, denoted by L_C, phase corresponding with the glacial phase by Cohen et al. was prepared by annealing the ordinary liquid, denoted by L_N, at 210 K, and different states in the L_C phase were formed by further annealing the prepared L_C-phase sample at 215 and 220 K. After the temperature jump from 210 to 215 K, two different processes first of heat absorption and then heat evolution were found to exist in the L_C phase. The first process showed reversible temperature dependence of the relaxation times near the temperature of L_C-phase formation as far as the process bringing the latter heat evolution effect did not proceed any further. The glass transition temperatures were found to be 209.9, 212.6, and 214.0 K for the L_C-phase samples formed at 210, 215, and 220 K, respectively. The fragility parameters of the respective samples were 104, 99, and 94, comparable with 104 in the L_N phase. The second process changed the relaxation times of the first process irreversibly to increase as the temperature of L_C-phase formation increases in the order of 210, 215, and 220 K. The temperature dependences of β-relaxation times were found to coincide completely with each other between the L_N and L_C phases. Those results were interpreted by the "intracluster rearrangement for α process" model combined with the "cluster structure for supercooled liquid and glass" model; the above second process corresponds to the increase/decrease in the size of the somehow "structurally ordered" region (named a cluster) and the first one to the order/disorder process of molecules within each cluster, namely the ordinary α process. The above second effect of heat evolution at 215 K is thus due to the development of ordering following the increase in the cluster size. The β relaxation would be attributed to the rearrangement of molecules between the clusters.

Introduction

Cohen et al. reported that triphenyl phosphite (hereafter abbreviated as TPP) has two amorphous phases; the amorphous phase newly found was denoted as glacial phase.[1] They observed similar X-ray diffraction patterns for the normally supercooled liquid and glacial phases. Since the discovery of the new amorphous phase, the properties of TPP have been examined by many research groups. Miltenburg and Blok[2] reported a heat capacity jump in the glass transition (giving rise to the transition temperature $T_{g\alpha} = 201.8$ K) for the normal liquid phase and an appreciable rise in the heat capacity curve in the region 200−227 K for the glacial phase formed by annealing the normal liquid at 217 K. The crystallization from the glacial to stable crystalline states was observed to occur at and above 227 K. Differential scanning calorimetry (DSC) has been adapted by Johari and Ferrari[3] and Wiedersich et al.[4] The glacial phase has been obtained only in the heating run at the rate ≤ 0.5 K min^{-1}. Dielectric properties have been studied by Schiener et al.,[5] Johari and Ferrari,[3] and Wiedersich et al.[4] The normal liquid has been found to show a rather remarkable non-Arrhenius behavior of the α-relaxation times and the presence of the β-relaxation process. For the glacial phase, it has been indicated that there exists a broad distribution of the α-relaxation times and that the average relaxation times shifts to higher temperature than that for the normal liquid. Hédoux et al. reported the low-frequency Raman spectra in the normal liquid, glacial, and crystalline states, and concluded that the spectrum of the glacial state corresponds to the perfect envelope of the phonon peaks observed in the crystal.[6] Through those works, Cohen et al.[1] and Johari and Ferrari[3] suggested that the glacial phase is a defect-ordered crystal and a plastic crystal, respectively, and Hédoux et al. indicated that the local order in the glacial phase is a very clear picture of the crystalline symmetry.[6] However, the details of the (normally supercooled liquid)-to-glacial phase transition and of the relaxation properties in the glacial phase have not been clarified yet and remain open to question as an interesting subject to be examined, and the all pictures given are only by speculation at present.

It has been discussed that supercooled liquids and glasses have heterogeneous structure due to the presence of certain structurally correlated regions at any moment. A strong/fragile concept proposed by Angell[7] on the basis of the non-Arrhenius property of relaxation times has greatly enhanced the scientific understanding of the structure and properties of liquids in relation to the heterogeneity and made many researchers become interested in the field of supercooled liquids and glasses. The structural correlation between molecules develops with decreasing temperature as a matter of course. In water, as an extreme

* Corresponding author. Phone and fax: +81-3-5734-2222. E-mail: moguni@chem.titech.ac.jp.

† Present address: Materials and Structure Laboratory, Tokyo Institute of Technology, 4529 Nagatsuta, Midori-ku, Yokohama 226-8503, Japan.

10.1021/jp983926q CCC: $18.00 © 1999 American Chemical Society
Published on Web 03/23/1999

example, a possibility has been long discussed that there might exist a transition between two supercooled liquid phases with different structures.[8−10] The two amorphous phases of TPP should also have different structures of molecular aggregation. The clarification of the difference is quite interesting for deep understanding of the relation between the development of structural correlation between molecules and the static and dynamic properties of supercooled liquids. The understanding would also help making any insight into the problem of liquid−liquid phase transition in water and so on.

The relaxation times of the molecular rearrangement have been long discussed in relation to the heterogeneous structure of the disordered molecular arrangement system. Essentially, two ideas have been proposed for the α process. One is represented by Adam and Gibbs (AG) theory.[11−14] Molecules at low temperatures form a cooperatively rearranging region (CRR) and the size of CRR increases toward infinity gradually with decreasing temperature under equilibrium. Thus, the relaxation times become long at low temperatures acceleratively resulting in the non-Arrhenius behavior. Each CRR might constitute a structurally correlated region and then the aggregation of the regions might give rise to a heterogeneous structure of the system at a moment. The point is that no distinction is made between a structured region and a cooperatively rearranging region. That is the reason the relaxation time is expressed by the configurational entropy of system in the theoretical framework.

The other is the "intracluster rearrangement for α process" model[15] combined with the "structured-cluster aggregation for supercooled liquid and glass" model.[16,17] In the model, a "structurally ordered", on the average, region is denoted by a cluster, and distinction is made between the cluster size and the rearranging unit of molecules within the cluster. The heterogeneous structure of the system is brought by the presence of the clusters, and the average cluster size increases with decreasing temperature under equilibrium. The α process corresponds to the order/disorder process of molecules within each cluster, and the rearrangement unit is rather independent of both the cluster size and the degree of molecular ordering within the cluster. The β process[16,18] corresponds to the rearrangement motion of molecules (without special arrangement structure) between clusters, and the rearrangement unit is recognized to be essentially the same as that of the α process.[15,16] The β relaxation times are expected to be rather independent of the molecular arrangement structures within clusters. The non-Arrhenius behavior of the α relaxation times is brought by increase in the activation energy for the α rearrangement motion with decreasing temperature due to development of the degree of molecular ordering within each cluster. The investigation of the molecular rearrangement processes in the two liquid phases of one compound, TPP, is expected to contribute to determining which of the proposed two ideas is appropriate to describe the molecular structure and rearrangement in liquids and glasses.

In the present study, high precision X-ray diffraction patterns were obtained again for the two liquid phases; the two phases are tentatively designated hereafter, based on the results of X-ray diffraction experiment, as L_N, indicating normally condensed liquid, and L_C, expressing highly correlated liquid. The L_C phase corresponds with the glacial one by Cohen et al.[1] Optical microscopic observation was also adapted to see whether the L_C phase is optically isotropic or not. Heat capacities were measured with an adiabatic calorimeter of a high-precision type in the temperature range 13−320 K. In the present measurements, the L_N-to-L_C phase transition and the spontaneous heat evolution/absorption effects due to glass transitions were followed in detail in addition to the precise heat capacity determination. Dielectric relaxation properties were examined in the low-frequency range to clarify the relations between the α and β relaxation times in each of the L_N and L_C phases and between the α or β relaxation times in the two phases.

Experiment

Sample Preparation. Triphenyl phosphite (TPP, $(C_6H_5O)_3P$ [102-02-0]), purchased from Kanto Chemical Co., Inc., was purified by distillation under reduced pressure. The purified sample was loaded, under an atmosphere of helium gas, into a calorimeter cell, a dielectric-measurement cell, an X-ray diffractometer cell, and an optical microscopic cell. The purity of the sample was determined to be 99.2 mol % by a calorimetric fractional-melting method with the van't Hoff equation[19] assumed to hold.

X-ray Diffractometry. X-ray diffractometry was carried out with a powder X-ray diffractometer (Mac Science M18XHF) by using Cu Kα line with additional voltage and electric current of 50 kV and 300 mA, respectively. All intensity data were collected between $2\theta = 10°$ and 40° at a scanning rate of 8° min^{-1} in step of 0.02°. The cell adapted for liquid sample to the apparatus was described elsewhere.[20] X-ray diffraction patterns were taken at a constant temperature of 210 K for all the samples: the L_N-phase sample a precooled rapidly from 330 K, the L_C-phase sample (b) obtained by holding the L_N phase sample (a) at 210 K for 3 days, and the crystalline-phase sample (c).

Optical Microscopy. The L_N-to-L_C phase transition was followed at 210 K by using an optical microscope. The detail of the apparatus was already reported.[21] The results obtained by Cohen et al.[1] were confirmed. The light intensity passing through the sample decreased during the transition proceeding and then recovered the initial one resulting in the transparent appearance of the sample.

Adiabatic Calorimetry. The mass of the sample loaded into a calorimeter cell was weighed to be 20.416 g (corresponding to 0.06580 mol). Heat capacities were measured in the temperature range 13−320 K by an intermittent heating method with an adiabatic calorimeter.[22] In the ordinary measurements, the initial equilibrium temperature ($T_{e,i}$) of the cell was determined in the former rating period of 9 min, a specified quantity of electrical energy (ΔE) was supplied into the cell to increase the temperature by 1.5−2 K, and the final equilibrium temperature ($T_{e,f}$) of the cell was again determined in the latter rating period of 9 min. The gross heat capacity of the cell was evaluated to be $\Delta E/(T_{e,f} - T_{e,i})$ at $T_{av} = (T_{e,i} + T_{e,f})/2$, and the latter temperature rating served as the former rating in the next set of heat capacity measurement. When spontaneous heat evolution or absorption appear due to glass and phase transitions, one observes the corresponding spontaneous temperature rise or fall, respectively, in the temperature rating period. The inaccuracy and imprecision of the heat capacities derived were estimated previously to be less than ±0.3% and ±0.06%, respectively.[22]

The L_C phase was prepared by holding the sample in the L_N phase at 210 K for 2 days. The enthalpy of the L_N-to-L_C phase transition was measured by keeping the sample in the L_N phase at the constant temperature and tracking the heat evolution due to the transition. The inner adiabatic shield was regulated at some lower temperature than the cell, and the temperature of the cell was kept constant by flowing electrical current through the heater wire for compensation of constant heat leak from

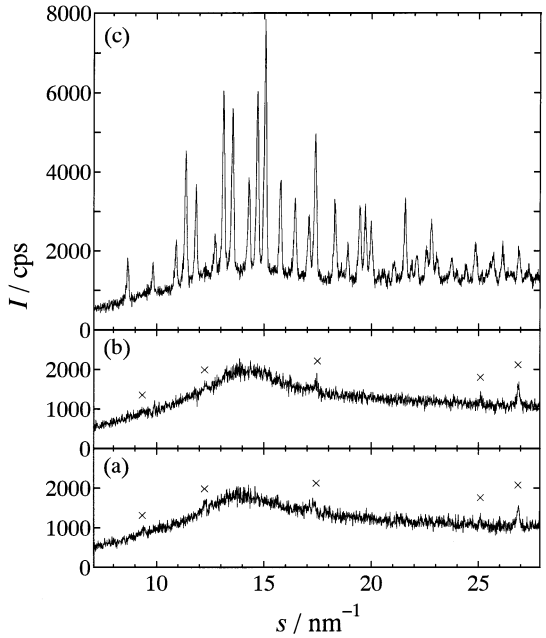

Figure 1. Powder X-ray diffraction patterns of triphenyl phosphite (TPP): (a) ordinary liquid, denoted by L_N; (b) highly correlated liquid, denoted by L_C, prepared by annealing the sample (a) at 210 K for 3 days; (c) crystal. The patterns were taken at 210 K, and the peaks marked by crosses originate from the sample cell including a beryllium film used.

the cell to the shield. The spontaneous heat evolution effect due to the transition was observed as the decrease in the current from the initial normal value without the transition. The enthalpy change in the L_C-phase sample after a temperature jump from 210 to 215 K was measured in the same way.

The equilibrium heat capacities in the L_C phase in the glass transition region were tried to be measured below the temperature at which the very L_C sample was prepared by holding. The rating of equilibrium temperature was then carried out by tracking the temperature drift for more than 20 h after the energy supply of 10 min.

Dielectric Measurements. The complex capacitance of the dielectric measurement cell containing TPP sample was measured as a function of temperature and frequency in the ranges 90−300 K and $0.1-10^6$ Hz, respectively, and the data were analyzed according to the capacitance (C) and loss tangent ($\tan\delta$) formalism. The measurements for the β-relaxation process were carried out by using an HP4284A impedance analyzer in the frequency range 10^2-10^6 Hz. The measurements for the α-relaxation process were carried out in a lower frequency range, $0.1-10^3$ Hz, by using an instrument in which a standard capacitor was connected in series to the sample as another capacitor and the output signal across the standard capacitor was detected with an EG&G DSP7260 lock-in amplifier reflecting the ac response of the sample.[23] This was because the experiment using a higher frequency range necessarily brought the sample to higher temperatures at which the sample had higher tendency to crystallize. In both the cases, an oscillating electric field applied to the cell was set at 1 V_{rms}. The detailed description of the apparatus will be given elsewhere. All the measurements were executed on heating the sample at a rate of 0.1 K min^{-1}.

Results

X-ray Diffraction Patterns. Figure 1 shows the powder X-ray diffraction patterns, taken at 210 K, of supercooled L_N-phase liquid (a), L_C-phase liquid (b), and crystal (c). The last, (c), gave many Bragg peaks indicative of the crystalline state. The former two, (a) and (b), being quite similar without any Bragg peak observed, on the other hand, showed only halo patterns characteristic of liquid and glass; a broad peak was found at $s = 14$ nm^{-1}. There have been two types of mesophases recognized so far between liquid and crystalline phases, namely, plastic crystal[24] and liquid crystal.[25] The former possesses three-dimensional long-range order with respect to the positions of molecules, resulting in a small number of Bragg peaks in the X-ray diffraction pattern. The pattern (b) of the L_C-phase indicates, in this sense, that the state of molecular aggregation cannot be characterized as a kind of plastic crystal. Among the latter liquid crystals, the nematic one has no long-range order with respect to the molecular positions but possesses a direction specific, as an average, to molecules on account of the slender shape of a molecule. In such cases, the X-ray diffraction patterns are rather similar to those of (b) in Figure 1 but with an additional broad peak at s corresponding to the inverse molecular length. The nematic liquid crystals are, on the other hand, optically anisotropic due to the presence of direction specific to the molecules. According to the results of light intensity passing through the L_N- and L_C-phase samples by Cohen et al.[1] and by the present microscopic observation, however, TPP in the L_C phase was optically isotropic. This indicates that the L_C phase cannot be characterized as a kind of liquid crystal. Thus, it follows that the state of molecular aggregation in the L_C phase must be classified as liquid at the present.

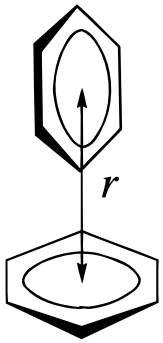

Figure 2. Orientational correlation often found between two phenyl groups in liquid and crystalline states of some compounds. r indicates the distance between the centers of phenyl groups.

The X-ray diffraction pattern (b) in Figure 1 shows a little higher intensity at around $s = 14$ nm^{-1} than (a) in the L_N phase; the peak intensity of the former amounts to 2000 cps compared with 1800 cps in the latter. This strongly indicates that some correlation with respect to the orientation of molecules develops in the L_C phase as referred to the L_N phase, though any specific direction does not arise in the whole liquid without slender or disklike character in the molecular shape. In this sense, the liquid generated by annealing the L_N-phase liquid at 210 K could be reasonably named a highly correlated liquid. The $s = 14$ nm^{-1}, at which the diffraction pattern gave a broad peak, corresponds roughly to 0.45 nm in the real space. This spacing is rather close to r, as illustrated in Figure 2. Such situations have been observed in the crystalline state of some compounds, which possess phenyl groups or similar aromatic rings[26,27] and are suggested to be present in the liquid state of benzene.[28,29] The structural correlation developed in the L_C phase might be thus connected to the arrangement of phenyl groups of TPP over the mesoscopic scale.

Heat Capacities. Figure 3 shows molar heat capacities obtained. The crystal, results of which are represented by open

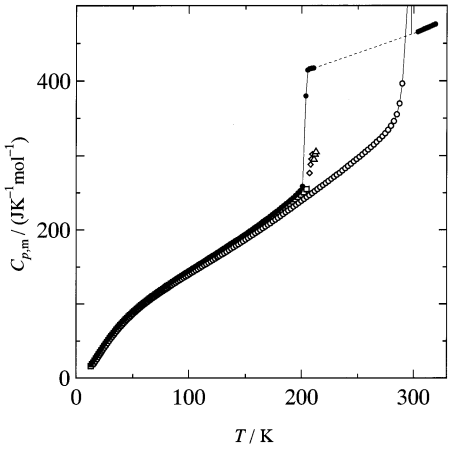

Figure 3. Molar heat capacities of TPP: (○) crystal; (●) L_N-phase liquid and glass; (□) L_C-phase glass; (◇) and (△) apparently equilibrium states of the L_C phase formed at 210 and 215 K, respectively.

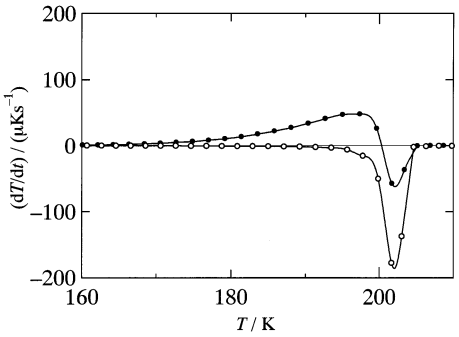

Figure 4. Temperature dependence of the rates of spontaneous temperature drifts observed in the L_N-phase sample: (○) precooled rapidly at 5 K min^{-1}; (●) precooled slowly at 13 mK min^{-1}.

circles, melted at (297.8 ± 0.2) K. Solid circles stand for the results of L_N-phase liquid and glass formed by rapid cooling of the liquid. A glass transition took place at around 200 K, and the associated heat capacity jump was estimated to be 155 J K^{-1} mol^{-1}. Figure 4 shows temperature dependence of the rates of spontaneous temperature drifts observed in the glass transition. In the sample precooled rapidly at 5 K min^{-1}, the spontaneous heat evolution effect started to appear at around 165 K, gave its maximum at around 195 K, and turned over to heat absorption effect at around 200 K. The drift returned to the normal one at around 205 K after yielding a maximum absorption effect at around 202 K. In the sample precooled slowly at 13 mK min^{-1}, on the other hand, only spontaneous heat absorption effect appeared with its maximum at around 202 K, and the drift returned to the normal one at 205 K. Such behaviors are reasonably understood as a glass transition[30] taking place at (200 ± 2) K which is a little lower than the temperature of maximum absorption rate found in the slowly precooled sample.

The first L_C-phase sample was prepared by annealing the L_N-phase sample at 210 K for 2 days after nucleation of the L_C-phase aggregate through precooling to 80 K. Figure 5 shows the spontaneous heat evolution effect observed due to L_N-to-L_C phase transition as a function of time in the range below 166 ks. The transition started to proceed at about 10 ks after setting the L_N-phase liquid at 210 K and showed its maximum rate at around 40 ks. The enthalpy of transition at 210 K was estimated by the integration of the effect with respect to time to be (7.0 ± 0.1) kJ mol^{-1}. The second L_C-phase sample was prepared by annealing the above-prepared L_C-phase sample at

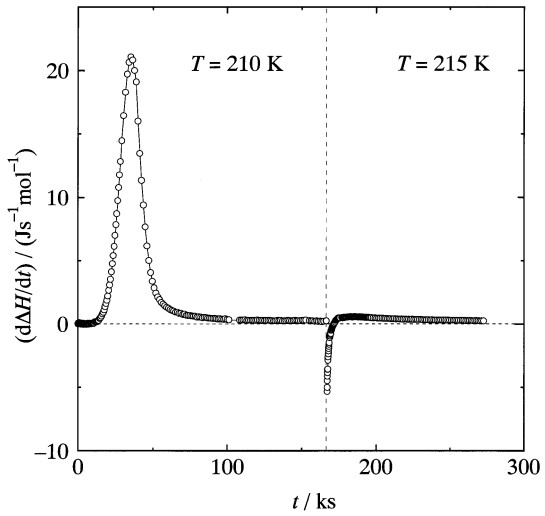

Figure 5. Time dependence of spontaneous heat evolution and absorption effects observed after setting the L_N-phase sample at 210 K. The heat evolution effect, as due to the L_N-to-L_C phase transition, started to be observed at around 10 ks with its peak at around 40 ks. The temperature of the sample was then increased from 210 to 215 K at 166 ks after apparent stabilization of the L_C phase at 210 K had been achieved. The heat absorption effect was accompanied by the temperature jump and was followed by a heat evolution effect around 180 ks.

215 K. Spontaneous heat absorption and subsequent heat evolution effects observed after the temperature jump are shown in Figure 5 in the time range 166−272 ks. Since the heat absorption effect appeared immediately after the temperature jump so that it was impossible to determine the normal electric current without any anomalous behavior of the sample at 215 K, the data were plotted tentatively so as to make the final data point of heat evolution at 215 K to coincide with that at 210 K. Therefore, it was impossible to determine the enthalpy change due to the temperature jump from 210 to 215 K. The most important point here is, however, that after the temperature jump, first heat absorption and then heat evolution (namely, heat-release) effects were observed as indicated by the appearance of the maximum in the plots at around 172 ks in Figure 5. This means that there exist definitely two rather independent processes proceeding after the jump and that the relaxation time of the heat absorption (namely entropy-increasing) process is comparatively short and the characteristic time of the process leading to the heat evolution effect (accordingly entropy-decreasing effect) is rather long.

Open squares in Figure 3 represent heat capacities of TPP in the glassy state of the L_C phase. The values are just between those of the L_N and crystalline phases. Open diamonds and triangles represent the apparent equilibrium heat capacities of L_C phases formed by annealing at 210 and 215 K, respectively. The heat capacities were measured only below the respective temperatures of L_C-phase formation and by following for 20 h the temperature drifts of heat absorption, which corresponds to the effect observed immediately after the temperature jump from 210 to 215 K at 166 ks in Figure 5. The drifts looked to have disappeared in 5−10 h after each energy input, though the heat evolution effect with a much longer time constant might have started to appear as the temperature approached that of L_C phase formation. The heat capacities derived would correspond to the apparently equilibrium ones including the heat absorption effect, but without the heat evolution effect, due to temperature rise. The heat capacity contribution increases rapidly, and thus, the configurational entropy decreases, with increasing temperature.

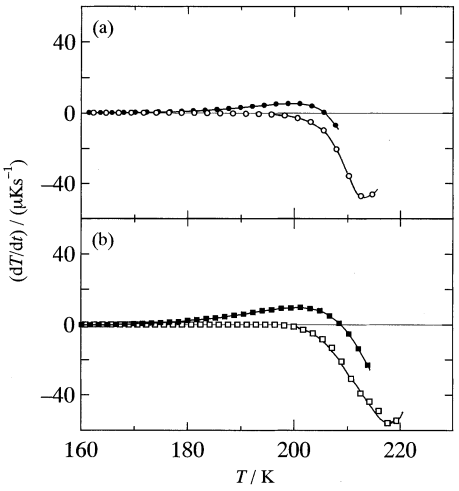

Figure 6. Temperature dependence of the rates of spontaneous temperature drifts observed on heating intermittently: (a) and (b) L_C-phase samples formed at 210 and 215 K, respectively; (●) and (○), precooled rapidly at 5 K min^{-1} and slowly at 18 mK min^{-1}, respectively, below 210 K; (■) and (□), precooled rapidly at 5 K min^{-1} and slowly at 18 mK min^{-1}, respectively, below 215 K.

But the temperature at which the contribution becomes remarkable depends on the temperature of L_C phase formation and increases as the latter temperature increases.

Parts a and b of Figure 6 show temperature dependence of the rates of temperature drifts due to spontaneous heat evolution/absorption effects, observed on heating intermittently the Lc-phase samples formed at 210 and 215 K, respectively. Filled circles and squares represent the results of the samples precooled rapidly from 210 and 215 K, respectively, and the samples showed exothermic and then endothermic temperature drifts in the heating direction. Open circles and squares represent the results of the samples precooled slowly below 210 and 215 K, respectively, and the samples showed rather only endothermic temperature drifts. These behaviors are just the thermal features observed in glass transitions.[30] The glass transition temperatures (T_g), at which the relaxation time (τ) becomes 1 ks, were estimated to be around 210 and 214 K for the L_C-phase samples formed by annealing at 210 and 215 K, respectively, from the empirical relation that the slowly precooled glass sample shows the maximum endothermic drift at a few K higher temperature than the T_g.

It is noticed that a glass transition phenomenon was observed around the temperature of L_C phase formation and that the glass transition temperature increased as the temperature of L_C phase formation increased. In general, the relaxation time becomes long when the degree of molecular ordering of some kind develops. The present results would mean that some kind of molecular ordering develops with increasing the temperature of L_C phase formation at least in the range 210−215 K.

α Process Observed by Dielectric Relaxation. Figure 7 shows temperature dependence of the capacitance, measured on heating at 0.1 K min^{-1}, at 0.1 Hz for the dielectric measuremet cell containing each sample; filled circles represent the results for the sample being in the L_N phase at 200 K before starting the measurement. The rise at around 207 K with increasing temperature is due to freezing-out of the α rearrangement of molecules found at a glass transition above by the calorimetry, and the fall beginning at around 217 K is attributed to the transition from the L_N to L_C phases. Open circles, squares, and diamonds represent the results for the samples in the L_C phase formed by annealing the L_N-phase

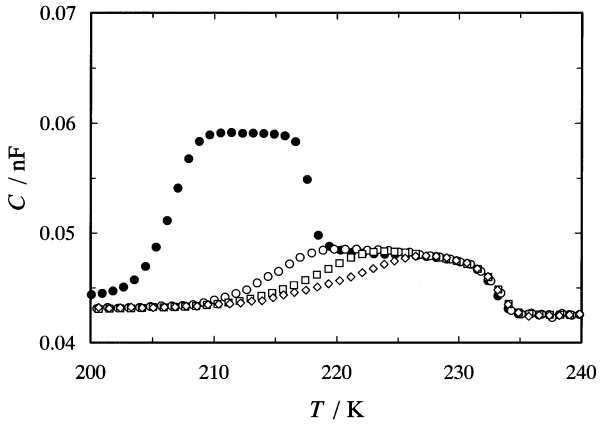

Figure 7. Temperature dependence of capacitance, measured on heating at 0.1 K min^{-1}, at 0.1 Hz for the dielectric measurement cell containing sample: (●) sample being in the L_N phase at 200 K; (○), (□), and (◇), samples being at 200 K in the L_C phase formed at 210, 215, and 220 K, respectively.

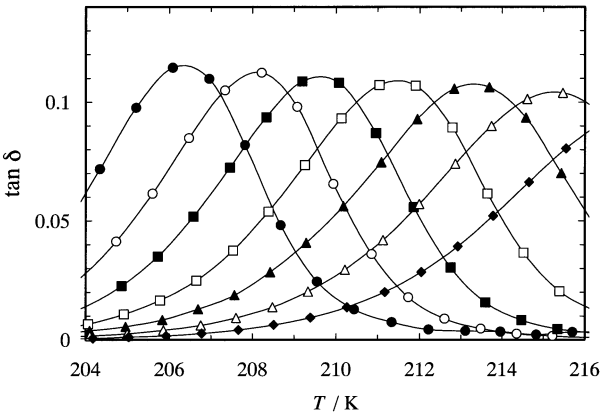

Figure 8. Temperature dependence of loss tangent (tan δ) at constant frequencies for the L_N phase: (●) 0.1 Hz; (○) 0.5 Hz; (■) 2 Hz; (□) 10 Hz; (▲) 46.4 Hz; (△) 200 Hz; (◆) 1 kHz.

sample at 210, 215, and 220 K, respectively, and precooled to 200 K. The respective rises at around 217, 220, and 223 K are due to freezing-out of the α rearrangement of molecules. All the samples showed the fall, starting at around 230 K, which was attributed to the crystallization. Thus, the L_N and L_C phases are judged to be rather stable below 217 and 230 K, respectively, under such a heating condition.

Figure 8 shows the results of temperature dependence of tan δ observed at some constant frequencies in the range $0.1-10^3$ Hz, on heating at 0.1 K min^{-1} for the L_N phase above the glass transition temperature (T_g) and below 216 K. Figure 9 shows the corresponding plot of frequency dependence of tan δ at some constant temperatures. The peak height exhibited a negligibly small tendency of decreasing with increasing temperature and the shape of tan δ vs log of frequency, log f, curve hardly changes with temperature. The temperature of the tan δ peak at each constant frequency in Figure 8 and the frequency of the tan δ peak at each constant temperature in Figure 9 are recognized as corresponding to the rate of molecular rearrangement at the temperature and are represented by open and closed circles, respectively, as Arrhenius plots in Figure 12, where the frequencies are converted to the relaxation times (τ) by a relation

$$\tau = 1/(2\pi f) \tag{1}$$

The relaxation times derived from the plots of tan δ of two kinds are in good agreement with each other. They were expressed

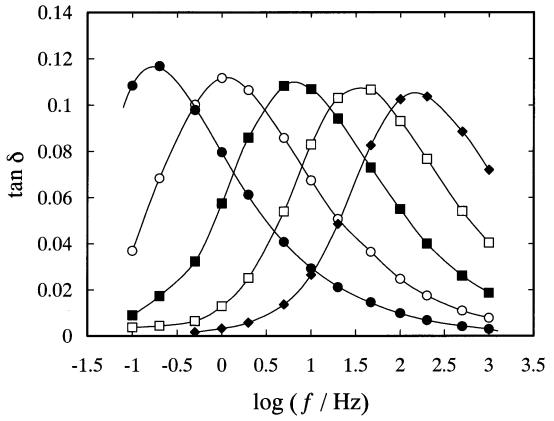

Figure 9. Frequency dependence of tan δ at constant temperatures for the L_N phase: (●) 207 K; (○) 209 K; (■) 211 K; (□) 213 K; (◆) 215 K.

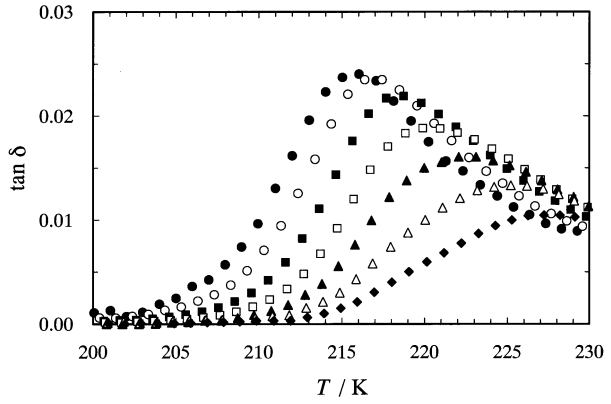

Figure 10. Temperature dependence of tan δ measured on heating, at 0.1 K min^{-1}, the L_C-phase sample formed at 210 K: (●) 0.1 Hz; (○) 0.4 Hz; (■) 2 Hz; (□) 10 Hz; (▲) 40 Hz; (△) 200 Hz; (◆) 1 kHz.

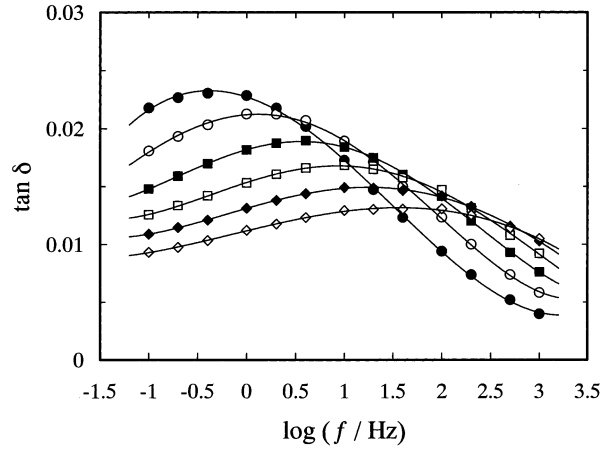

Figure 11. Frequency dependence of tan δ for the L_C-phase sample formed at 210 K: (●) 218 K; (○) 220 K; (■) 222 K; (□) 224 K; (◆) 226 K; (◇) 228 K. Data of tan δ were obtained on heating the sample at 0.1 K min^{-1}, and then the values at each constant temperature were estimated by interpolation of the data as functions of temperature at the respective frequencies.

in terms of the following Vogel−Tamman−Fulcher (VTF)[31] equation by fitting:

$$\tau = A \exp\{B/(T - T_0)\} \quad (2)$$

where $A = 4.2 \times 10^{-27}$ s, $B = 3837$ K, and $T_0 = 143.7$ K. The fragility parameter (m) as given by a following expression[7] was evaluated to be 104:

$$m = \mathrm{d}(\log \tau)/\mathrm{d}(T_g/T)|_{T=T_g} \quad (3)$$

Figure 10 shows the temperature dependence of tan δ observed, at constant frequencies in the range $0.1-10^3$ Hz, on heating at 0.1 K min^{-1} the sample in the L_C phase formed by annealing at 210 K. Figure 11 shows the corresponding plots of frequency dependence of tan δ at constant temperatures. The peak height decreased appreciably with increasing the temperatures. In view of the fact that the static dielectric constant did not change so much with temperature in the relevant range as shown in Figure 7, this indicates that the shape of the tan δ vs log f curve changes appreciably to get the frequency distribution broadened with increasing temperature. Filled and open squares in Figure 12 represent, as Arrhenius plots, the relaxation times derived from the points of tan δ maximum in the tan δ vs T curves in Figure 10 and from tan δ vs log f curves in Figure 11, respectively. The relaxation times derived by the two methods differ considerably from each other at higher temperatures and are rather close to each other only at around the low-temperature limit measured. Such observations are understood to be attributed to the change in the state of molecular aggregation with increasing temperature as the thermal properties of the two L_C-phase samples formed at 210 and 215 K were different from each other. In this sense, only the relaxation times at low temperatures at which the two kinds of data, represented by open and filled squares, are in agreement with each other are meaningful as properties for some specific state of molecular aggregation. The separation between the two sets of data from tan δ vs T and tan δ vs log f curves indicates that any change in the state of molecular aggregation is under progress in the L_C-phase sample during the constant-rate heating. In such a situation, the relaxation time data from tan δ vs log f curves are meaningful rather than those from tan δ vs T curves, since the tan δ data were then derived as those at constant temperature, namely more or less at constant state of molecular aggregation. Open triangles and diamonds in Figure 12 represent the results from tan δ vs log f curves of the L_C-phase samples formed by annealing at 215 and 220 K, respectively. While the state of molecular aggregation changes with increasing temperature, the three different sets of data of the L_C-phase samples rather coincide with one another at the high-temperature limit indicating that the samples approach the same state there in such a condition of the heating rate of 0.1 K min^{-1} above the temperature of L_C-phase formation.

Figure 13 shows, on an Arrhenius plot, the relaxation times derived in the conditions that the peak height in the tan δ vs log f curve changed negligibly with temperature and that the same relaxation times were obtained from tan δ vs T and tan δ vs log f curves. The conditions indicate no appreciable progress of the complicated change in the state of molecular aggregation in the range where the data are plotted. Filled and open marks represent the results from the former and latter curves, respectively, and squares, triangles, and diamonds stand for the results of the L_C-phase samples formed at 210, 215, and 220 K, respectively. An open circle represents the result at 220 K from the tan δ vs log f curve of the L_C-phase sample (denoted here as sample A) formed at 210 K and heated at 0.1 K min^{-1} up to 220 K, and filled circles show the results from tan δ vs T curves of the sample obtained by quenching the sample A quickly to low temperature below 210 K after the measurement at the 220 K. Thus, the open and filled circles are recognized to give the properties of the sample in the same state of molecular aggregation in a certain sense. Four different samples showed temperature dependence of relaxation times rather parallel to one another, indicating that the dependence is a real property

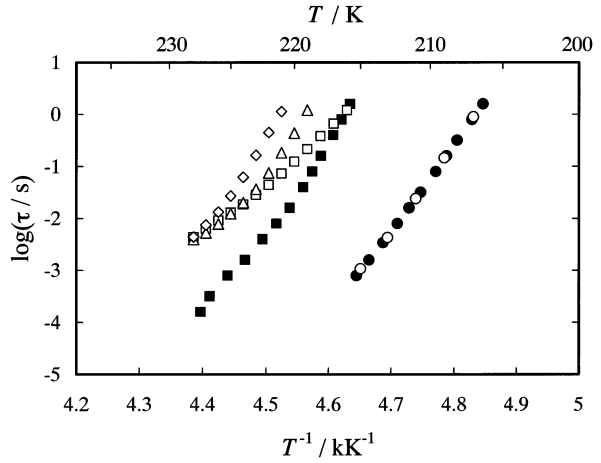

Figure 12. Arrhenius plot of relaxation times derived as sets of temperature (T) and frequency (f) at which peaks in the tan δ, against T and log f, curves were observed: (●) from the temperature dependence for the L_N phase; (○) from the frequency dependence for L_N phase; (■) and (□) from the temperature and frequency, respectively, dependence for the L_C-phase sample formed at 210 K; (△) and (◇) from the frequency dependence for the L_C-phase samples formed at 215 and 220 K, respectively. The frequency was converted to relaxation time by a relation, $\tau = 1/(2\pi f)$.

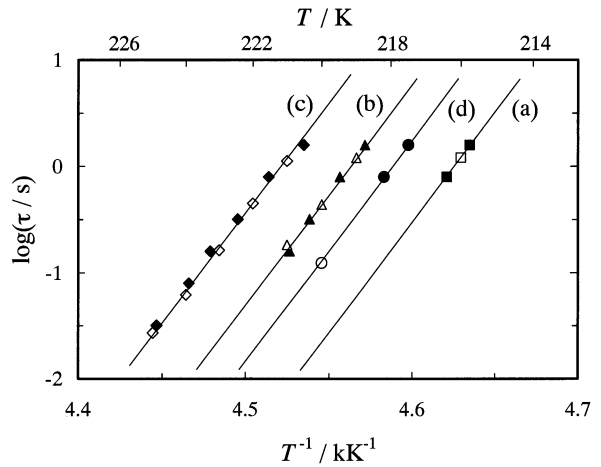

Figure 13. Arrhenius plot of relaxation times for the L_C-phase samples: filled marks, from temperature dependence; open marks, from frequency dependence; (■) and (□) , sample formed at 210 K; (○) sample A heated at 0.1 K min^{-1} up to 220 K after having formed the L_C phase at 210 K; (●) sample prepared by quenching the sample A from 220 K down to 210 K; (▲) and (△) sample formed at 215 K; (◆) and (◇) sample formed at 220 K. Straight lines a−d were obtained by fitting to the both of filled and open marks for the respective samples.

for each specific state of molecular aggregation. The glass transition temperatures were determined, by extrapolating linearly the inverse temperature dependence of the relaxation times as indicated by solid lines (a−c), to be 209.9, 212.6, and 214.0 K for the three L_C-phase samples formed at 210, 215, and 220 K, respectively. The respective fragility parameters (m) were estimated to be about 104, 99, and 94. Such large values of the parameters strongly support the recognition that the process proceeding is the α process in the L_C phase.

Two points should be noticed here. The first point is that, as the temperature at which the L_C phase is formed increases, the temperature of L_C phase formation and the glass transition temperature of a thus-formed L_C-phase sample become more separate; the latter temperature is lower than the former. This means that there exist two somewhat independent processes in the L_C phase; namely, one proceeds rather irreversibly with

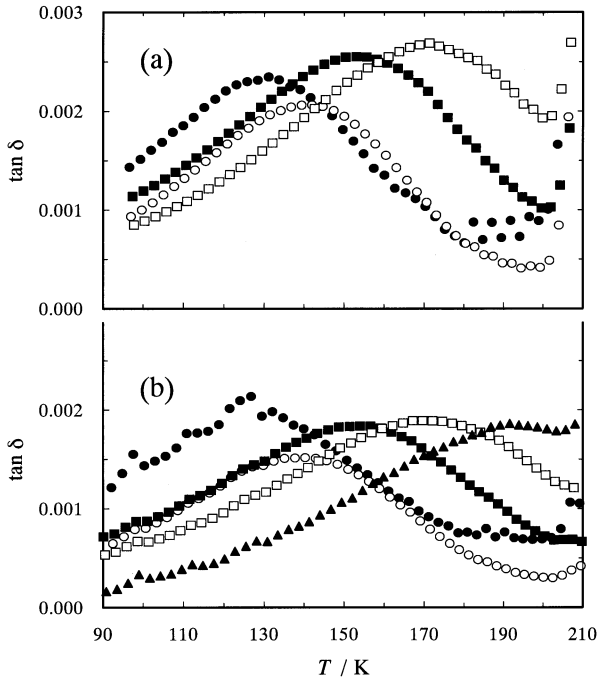

Figure 14. Temperature dependence of tan δ for β-relaxation process: (a) L_N phase; (b) L_C phase; (●) 383 Hz; (○) 2.73 kHz; (■) 19.2 kHz; (□) 150 kHz; (▲) 1 MHz. The difference in the magnitude of tan δ between different frequencies appeared as ascribed to frequency dependence of the sensitivity of the impedance analyzer used, since the dielectric loss due to the β-relaxation was very small.

increasing temperature above that of L_C phase formation and the other shows a glass transition around the temperature of L_C phase formation and has the temperature dependence of its relaxation times given in Figure 13. The latter and former processes correspond to those resulting in the heat absorption and heat evolution effects, respectively, after the temperature jump from 210 to 215 K in Figure 5. The relaxation times of the former process should be the same in the order of magnitude, 10^4 s, at each temperature of L_C phase formation after the respective long stabilization. As the structure with respect to the former process develops, the characteristic times of the two processes become separate due to the decrease in the glass transition temperature of the latter process referred to the temperature of L_C phase formation. The second point is that the fragility of relaxation times comes out from the development of structural ordering with respect only to the latter process. The magnitude of the fragility is comparable with that, 104, of the L_N-phase liquid.

***β* Process Observed by Dielectric Relaxation.** Parts a and b of Figure 14 show temperature dependence of tan δ observed below 210 K in the L_N and L_C phases, respectively. The dependence at each constant frequency exhibits definitely a peak, indicating that the β-relaxation process[16,18] in addition to the α process observed above 210 K is present in the both phases. The set of the frequency and temperature as showing the tan δ peak is interpreted to give the relaxation time (τ) of the process by the relation (1) at the temperature. Figure 15 shows the Arrhenius plots of the relaxation times together with those of the α process. Open and filled squares stand for the results of the β-relaxation times in the L_N and L_C phases, respectively, and open and filled circles for those of the respective α processes. The β-relaxation times and their temperature dependence are essentially in complete agreement between the two phases while those of the α processes are considerably different. This would mean that the β processes are essentially the same

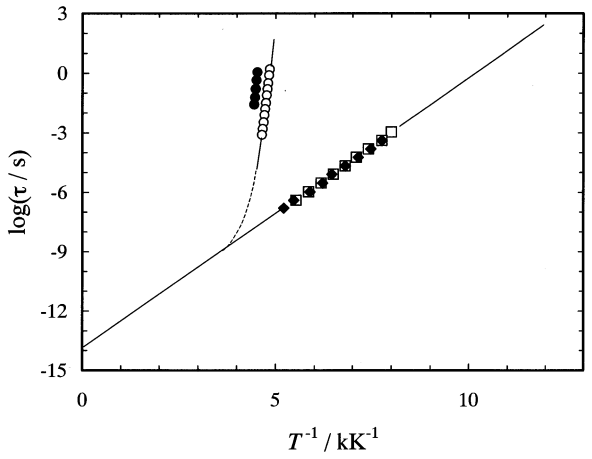

Figure 15. Arrhenius plot of relaxation times: (○) and (□) α- and β-relaxation times, respectively, for L_N phase; (●) and (◆) α- and β-relaxation times respectively for the L_C phase.

in the two liquid phases. The temperature dependence was expressed by the Arrhenius equation

$$\tau = \tau_0 \exp\{\Delta\epsilon_{a,\beta}/(RT)\} \quad (4)$$

where $\tau_0 = 1.2 \times 10^{-14}$ s and $\Delta\epsilon_{a,\beta} = 26.1$ kJ mol^{-1}. The τ_0 value is of the same order of magnitude as we have expected[15,16] and is reasonable as the inverse of the frequency of molecular vibration.

Discussion

Characteristics of the State and Its Change of Molecular Aggregation in the L_C Phase of TPP. The L_C phase was tentatively characterized to be a liquid phase possessing more developed structural correlation than the L_N phase, though there remains a possibility that the L_C phase is a kind of crystalline phase with large lattice constants as suggested by some research groups.[1,3] In any case, the L_C phase is in the highly disordered state with respect to the molecular configuration. Three essential points have been disclosed concerning the structural characteristics and relaxation processes. The first point is that there exist two frozen-in processes in the L_C phase. The two processes appeared clearly in the spontaneous heat absorption/evolution effects as a function of time after the sudden temperature rise from 210 to 215 K as shown in Figure 5. The sample in the L_C phase had been kept at 210 K for 166 ks so as to reach the apparently equilibrium state before the jump. Let us denote the first process, which appeared as giving rise to the heat absorption effect, as process 1 and the second process, which appeared in the later time as giving rise to the heat evolution effect, as process 2; the former process has apparently shorter relaxation time than the latter. Assuming that the heat absorption and evolution effects correspond to the increase and decrease, respectively, in the configurational entropy of system, the situation observed is understood as illustrated in Figure 16. Curves a and b represent the temperature dependence of configurational entropy for the L_C-phase samples which have been formed at 210 and 215 K, respectively, and are in the apparently equilibrium state with respect to the process 1 under the nonequilibrium frozen-in state with respect to the process 2. Curve c represents the dependence expected for the sample being in the equilibrium state with respect to the two processes. While the L_N-phase sample is kept at 210 K for a long time, the whole sample transforms to the L_C phase but the relaxation time (τ_2) of the process 2 becomes long with time so that the

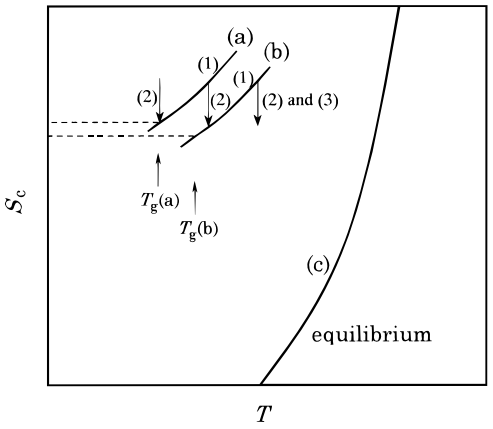

Figure 16. Schematic temperature dependence of configurational entropy in the different states of the L_C phase: (1) and (2), processes taking place in the L_C phase; lines a and b, the dependence under equilibrium with respect to process 1 but in the frozen-in state with respect to process 2 for the samples formed at 210 and 215 K, respectively; line c, the dependence under equilibrium with respect to the both processes 1 and 2; (3), crystallization process. Broken lines represent the frozen-in states with respect to the both processes 1 and 2. See text for the detail.

state of molecular aggregation with respect to the process 2 should be frozen in at some stage. When the temperature increases, as an example, from 210 to 215 K, the τ_2 gets short due to the temperature effect and some kind of ordering concerning the process 2 develops again as evidenced by the appearance of heat evolution at 215 K in the later time after the jump from 210 K in Figure 5. The process proceeding corresponds to a solid line (2) with arrow drawn from line a to line b in Figure 16. The state of molecular aggregation with respect to the process 2 is frozen in some other nonequilibrium state with $\tau_2 \sim 10^4$ s again. If the temperature of the system increases further, say to 220 or 230 K, as well as the state of molecular aggregation concerning the process 2 gets another frozen-in nonequilibrium state with gradually approaching the wholly equilibrium state with lower entropy, another process 3 of crystallization proceeds. The process 1 seems to show apparently reversible equilibrium properties depending on the state of molecular aggregation with respect to the process 2. The dependence is shown by the different temperature dependence of configurational entropy between the lines a and b in Figure 16. There definitely appeared calorimetric glass transition and dielectric dispersion phenomena with respect to the process 1. The frozen-in states of configurational entropy are represented by horizontal, broken lines in Figure 16. The glass transition temperatures (T_g(a) and T_g(b)) decrease relative to the respective temperatures of L_C phase formation, as the latter temperature indicated by a solid line (2) with arrow increases. All these facts indicate that the two processes affecting the state of molecular aggregation certainly exist in the L_C phase.

The second point is that the relaxation times of the process 1 show fragile property. Solid lines a and b in Figure 17 stand for schematic temperature dependence observed of relaxation times for the L_C-phase samples formed at 210 and 215 K, respectively, and dashed lines a′ and b′ stand for the corresponding dependence of presumed strong liquids with constant activation energies given at the respective glass transition temperatures. The real fragile property is understood to originate from the decrease in the activation energies with increasing temperature.[15,17] In view of the fact that the dependence of (a) and (b), namely the fragile property, was observed under some constant frozen-in state with respect to the process 2 in Figure

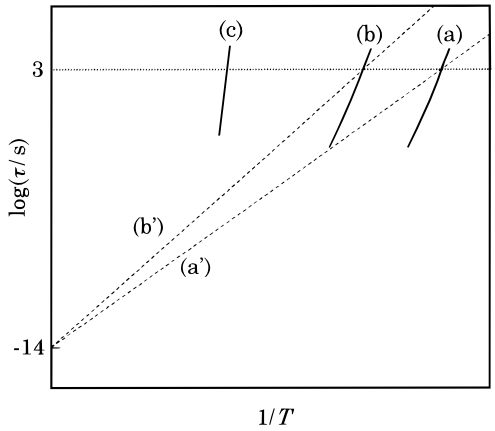

Figure 17. Schematic temperature dependence of relaxation times, on an Arrhenius plot, of the α process in the different states of the L_C phase: lines a, b, and c, states corresponding to the respective lines in Figure 16; (a′) and (b′), temperature dependence expected for strong liquids with activation energies given at the glass transition temperatures of (a) and (b), respectively.

16, the fragility property is understood to be caused by the change in the activation energies for the molecular rearrangement process 1 with temperature, namely, with the degree of ordering with respect to the process 1. Further, in view of the fact that the fragility parameter observed was comparable with that in the L_N phase, the temperature dependence of the state concerning the process 1 would be dominant in determining the fragility parameter for liquids being in the equilibrium state also with respect to the process 2. Solid line c in Figure 17 represents the temperature dependence of relaxation times expected for the L_C-phase liquid under equilibrium both in the respect to the processes 1 and 2. The fragility parameter would be somewhat larger than those of (a) and (b).

The third point is that the β-relaxation times are rather independent of the details of molecular arrangement and rearrangement rate concerning the α process. As shown in Figure 15, the α-relaxation times of the L_N and L_C phases are quite different, indicating that the details related to the α processes differ considerably, but the temperature dependence of β-relaxation times is completely in agreement between the two phases.

Structure and Relaxation Times in the L_C Phase as Interpreted Consistently with "Intracluster Rearrangement for α Process" Model. The present results are consistently interpreted by the picture given above in the Introduction as the "intracluster rearrangement for α process" model[15] combined with the "cluster structure for supercooled liquid and glass" model.[16,17] Figure 18 illustrates the cluster structure of liquid and the degree of molecular ordering within the clusters; the darkness of the region representing the cluster indicates the increased degree of the ordering. Process 1 is the rearrangement motion of a few molecules within each cluster, and process 2 is the process to change the cluster size. Figure 18a is the schematic illustration of the L_C phase formed at 210 K. As the relaxation time of process 2 reaches $\sim 10^4$ s, the clusters stop effectively progressing at some nonequilibrium state before reaching the equilibrium size realized on the line c in Figure 16 and the molecules within each cluster take some ordered arrangement determined by the cluster size and temperature. Figure 18b illustrates the situation realized at the time a little after the temperature jump to 215 K. Since the relaxation time of process 1 is assumed to be shorter than that of process 2, the molecules within each cluster take their degree of ordering corresponding to that at 215 K while the cluster size remains

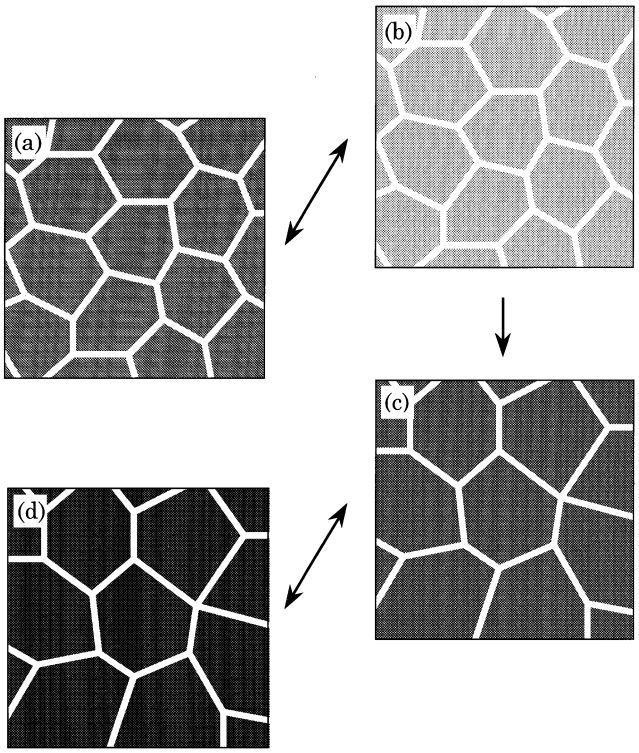

Figure 18. Schematic illustration of the cluster structure and the degree of order of molecular arrangement within clusters in the L_C-phase samples formed: (a) apparently equilibrium state formed at 210 K; (b) the state at the time a little after the jump from 210 to 215 K; (c) apparently equilibrium state at 215 K; (d) the state formed by cooling the sample c to 210 K. The states a and b are located on line a in Figure 16, and (c) and (d) on the line b. Therefore, the cluster size in the former states is smaller than that in the latter. The darkness of cluster represents the developed degree of order of molecular arrangement in each cluster. The shade gets dark, from (b) to (a) or from (c) to (d), with decreasing temperature under equilibrium with respect to process 1 in Figure 16, and it does, from (b) to (c), with increasing cluster size through process 2 in Figure 16.

constant as formed at 210 K. The degree decreases as a matter of course, and a heat absorption effect corresponding to the increase in the configurational entropy is observed. The process between the states shown in parts a and b of Figure 18 is reversible so that the glass transition phenomenon appears below the temperature due to the freezing-in of the molecular rearrangement process 1, as was observed. When the sample shown in Figure 18b is kept at 215 K for a longer time, the cluster size increases since the relaxation time of process 2 would be 10^2-10^3 s. As the cluster size increases, however, the molecular ordering correspondingly progresses due to the increase in the intermolecular interaction within the cluster and the heat evolution effect is observed. This process is illustrated as the change between the states shown in parts b and c of Figure 18 and proceeds irreversibly toward the state on the line c in Figure 16. As the cluster size increases, the relaxation time (τ_2) of process 2 becomes long. As the degree of molecular ordering increases within the cluster, the relaxation time (τ_1) of process 1 becomes long. Thus, the increase in the cluster size at 215 K stops again at some stage where $\tau_2 \approx 10^4$ s, and the temperature dependence of relaxation times of process 1 moves from line a to line b in Figure 17 resulting in the increase in the glass transition temperatures from T_g(a) to T_g(b) in Figure 16. The change between the states illustrated in parts c and d of Figure 18 corresponds to the reversible ordering/disordering of molecular arrangement with respect to the process 1 within the clusters while the cluster size remains constant. The temperature

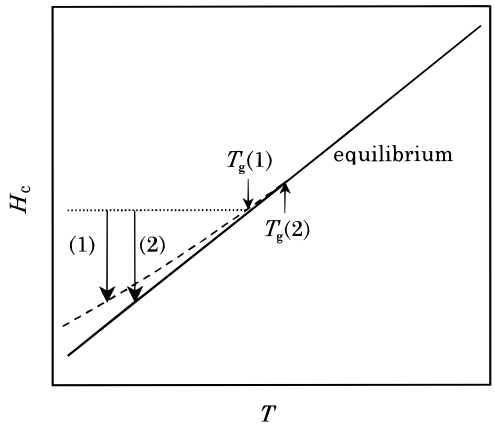

Figure 19. Calorimetric situation expected for disordered molecular arrangement systems in the glass transition region: (1) order/disorder process of molecules within cluster; (2) process to change the cluster size; $T_g(1)$ and $T_g(2)$, the glass transition temperatures due to freezing-in of the processes 1 and 2, respectively. The progress of process 2 is calorimetrically observed as the enthalpy change due predominantly to progress of order/disorder process 1 as responding to the change of cluster size.

dependence of the relaxation times (τ_1) is represented by line b in Figure 17. The change of the states from part a to part d of Figure 18 is hardly feasible because of the τ_2 being too long at 210 K as referred to our experimental time scale. The reverse change of the states from part a to part d of Figure 18 never occurs since the latter state (a) is unstable in the respect of the Gibbs energy compared with the former (d). As described above, the presence of two frozen-in processes concerning the α-molecular rearrangement process is reasonably interpreted by the model, and the heat absorption and evolution effects originate from the disordering and ordering, respectively, in the molecular arrangement within clusters. The change in the cluster size through the process 2 is considered to affect just the apparently equilibrium degree of molecular ordering within each cluster at the respective temperatures.

Calorimetric Properties Generally Expected for Disordered Molecular Arrangement Systems. The calorimetric and dielectric behaviors observed in the L_C phase of TPP were consistently interpreted above by the picture of the "cluster structure" model. In view of the fact that the L_C phase is in the disordered molecular arrangement state, the picture is judged to hold for any disordered system such as near-equilibrium liquid. Figure 19 illustrates the relation between the configurational enthalpy and temperature in the glass transition region. The solid line represents the configurational enthalpy under equilibrium with respect to two parameters; one parameter is the degree of order of molecules within each cluster, and the other parameter is the average cluster size, in reality the distribution of cluster sizes. In true equilibrium, the cluster sizes are determined by temperature and the degree of order so as to minimize the Gibbs energy of liquid system, and the degree of order within clusters is determined by each size of cluster and temperature. As the temperature decreases, according to the results of TPP, the cluster size is first frozen in at a glass transition temperature ($T_g(2)$) in Figure 19 and then the order/disorder process of molecules within each cluster is frozen in at another glass transition temperature ($T_g(1)$) in the figure. The liquid is really in the glassy state below $T_g(1)$ as represented by a dotted line in Figure 19. Between $T_g(1)$ and $T_g(2)$, it is in the equilibrium state with respect to the arrangement of molecules within cluster but in the nonequilibrium, frozen-in state with respect to the cluster size as represented by a dashed line in the figure. Since the calorimetry observes rather only the change in the degree of molecular order in the system, the calorimetric glass transition is observed at $T_g(1)$ and the calorimetric effect at $T_g(2)$ is expected to be rather small. Below the $T_g(1)$, two relaxation processes proceed; process 1 is the ordering/disordering in the molecular arrangement rather at constant cluster size as indicated by a solid line (1) with an arrow, and process 2 is the change in the cluster size. In fact, the change in the degree of molecular ordering as a response to the change in the cluster size is calorimetrically observed as indicated by a solid line (2) with an arrow.

The reason $T_g(2)$ is generally higher than $T_g(1)$ in liquids would be that the intercluster interaction, namely the driving force for the process 2 to proceed, would be rather weak compared with the intermolecular interaction within each cluster. However, we have previously found that the crystal nucleation proceeds even much below the α-glass transition temperature.[32] When a crystal embryo/nucleus is recognized as a kind of ordered cluster, the crystal nucleation, namely the enlargement of the cluster, is considered to proceed through the process 2 and thus, according to the above model, through the β-process which is the rearrangement of molecules between clusters. Therefore, the process 2 kinetically proceeds only if the temperature is above the β-glass transition temperature. In view of the fact that the Gibbs energy of the crystalline state is much lower than that of the liquid state, even though the molecular arrangement is rather in the disordered state as referred to that of complete crystal, the driving force for the crystal nucleation to proceed is much stronger than that for the enlargement of the cluster in the liquid state to occur. This would be the reason process 2 proceeds toward the crystalline state even below $T_g(2)$. On the other hand, if the liquid cluster enlarges below $T_g(1)$ as is kinetically feasible through the β process as well, the molecules in the enlarged region should remain rather in the low degree of order in the molecular arrangement, due to the relaxation time of process 1 being too long, resulting in a higher state in the Gibbs energy of system. Therefore, such a process is expected not to proceed as an event in the liquid state.

Conclusion

An L_C-phase sample was prepared by annealing the L_N-phase sample at 210 K, and other L_C-phase samples were formed by annealing the obtained L_C-phase sample at 215 and 220 K. It was found that the L_C-phase samples thus formed were in the nonequilibrium state. The most remarkable finding is that there exist two relaxation processes in the phase. The two processes were consistently interpreted by the "intracluster rearrangement for α process" model combined with the "cluster structure for supercooled liquid and glass" model; one is the order/disorder process of molecules within each "structurally ordered" cluster, and the other is the process which changes the cluster size. The relaxation time of the latter process was found to be effectively longer than that of the former. Therefore, the annealing at higher temperatures brought the L_C-phase sample into a more ordered state, namely with larger cluster size, and a glass transition in correspondence with each average cluster size was observed with respect to the order/disorder of molecular arrangement within the cluster. The good consistency of the model with the experimental facts strongly supports a picture of the model for structure and rearrangement of molecules in supercooled liquid and glass.

According to the model, different structures potentially appear for the molecular arrangement within the clusters. As a matter of course, for each liquid with different structure to exist as a

different phase, the structure should be stabilized by some cooperative structural interaction through a decrease in the interfacial energies between the clusters. Such a situation gives rise to a possibility of a liquid−liquid phase transition. Though the equilibrium stable state of the L_C phase was not obtained and therefore two equilibrium stable liquid phases were not realized in TPP, the equilibrium phase transition would be found between liquid phases in some compound in the future.

At the present, it is difficult to determine the liquid structure with respect to the molecular arrangement including the disorders allowed. Such works are especially desired as the future research subject and also in order to confirm whether the model supported in the present study is really correct or not.

Acknowledgment. This work was partly supported by a Grant-in-Aid for Scientific Research (Grant 10440169) from the Ministry of Education, Science, Sports and Culture, Japan.

References and Notes

(1) Cohen, I.; Ha, A.; Zhao, X.-L.; Lee, M.; Fischer, T.; Strouse, M. J.; Kivelson, D. *J. Phys. Chem*. **1996**, *100*, 8518. Ha, A.; Cohen, I.; Zhao, X.-L.; Lee, M.; Kivelson, D. *J. Phys. Chem*. **1996**, *100*, 1.

(2) Miltenburg, K. van; Blok, K. *J. Phys. Chem*. **1996**, *100*, 16457.

(3) Johari, G. P.; Ferrari, C. *J. Phys. Chem.* **1997**, *101*, 10191.

(4) Wiedersich, J.; Kudlik, A.; Gottwald, J.; Benini, G.; Roggatz, I.; Rössler, E. *J. Phys. Chem.* **1997**, *101*, 5800.

(5) Schiener, B.; Loidl, A.; Chamberlin, R. V.; Böhmer, R. *J. Mol. Liq.* **1996**, *69*, 243.

(6) Hédoux, A.; Guinet, Y.; Descamps, M. *Phys. Rev.* **1998**, *B58*, 31.

(7) Angell, C. A. *J. Non-Cryst. Solids* **1985**, *73*, 1; *J. Non-Cryst. Solids* **1991**, *131*−*133* , 13.

(8) Mishima, O.; Calvert, L. D.; Whalley, E. *Nature* **1985**, *314*, 76. Whalley, E.; Klug, D. O.; Handa, Y. P. *Nature* **1989**, *342*, 782.

(9) Angell, C. A. *J. Phys. Chem*. **1993**, *97*, 6339.

(10) Speedy, R. J. *J. Phys. Chem*. **1992**, *96*, 2322.

(11) Adam, G.; Gibbs, J. H. *J. Chem. Phys*. **1965**, *43*, 139.

(12) Donth, E. *J. Non-Cryst. Solids* **1982**, *53*, 325.

(13) Moynihan, C. T.; Schroeder, J. *J. Non-Cryst. Solids* **1993**, *160*, 52.

(14) Hodge, I. M. *J. Non-Cryst. Solids* **1991**, *131*−*133*, 435.

(15) Oguni, M. *J. Non-Cryst. Solids* **1997**, *210*, 171; *Kobunshi Ronbunshu (J. Polym. Sci. Technol.)* **1996**, *53*, 636.

(16) Fujimori, H.; Oguni, M. *Solid State Commun*. **1995**, *94*, 157.

(17) Mizukami, M.; Fujimori, H.; Oguni, M. *J. Phys. Condens. Matter* **1995**, *7*, 6747.

(18) Goldstein, M. *J. Chem. Phys*. **1969**, *51*, 3728. Johari, G. P. *Lect. Notes Phys*. **1987**, *227*, 90.

(19) Tunnicliff, D. D.; Stone, H. *Anal. Chem*. **1955**, *27*, 73.

(20) Hikima, T.; Hanaya, M.; Oguni, M. *J. Non-Cryst. Solids* **1998**, *235*−*237*, 539.

(21) Hikima, T.; Adachi, Y.; Hanaya, M.; Oguni, M. *Phys. Rev.* **1995**, *B52*, 3900.

(22) Fujimori, H.; Oguni, M. *J. Phys. Chem. Solids* **1993**, *54*, 271.

(23) Kim, B. G.; Kim, J. *Phys. Rev*. **1997**, *B55*, 5558.

(24) Sherwood, J. N. *The Plastically Crystalline State*; Wiley: New York, 1979.

(25) McMillan, W. L. *Phys. Rev.* **1973**, *7*, 1419.

(26) Abrahams, S. C.; Lipscomb, W. N. *Acta Crystallogr*. **1952**, *5*, 93.

(27) Andre, D.; Figuiere, P.; Fourme, R.; Ghelfenstein, D.; Labarre, D.; Szwarc, H. *J. Phys. Chem. Solids* **1984**, *45*, 299.

(28) Hobza, P.; Selzle, H. L.; Schlag, E. W. *J. Am. Chem. Soc*. **1994**, *116*, 3500.

(29) Narten, A. H. *J. Chem. Phys*. **1968**, *48*, 1630.

(30) Suga, H.; Seki, S. *J. Non-Cryst. Solids* **1974**, *16*, 171; *Faraday Discuss.* **1980**, *69*, 221.

(31) Vogel, H. *Phys. Z.* **1921**, *22*, 645. Fulcher, G. S. *J. Am. Ceram. Soc*. **1925**, *77*, 3701. Tammann, G.; Husse, G. *Z. Anorg. Allg. Chem*. **1926**, *156*, 245.

(32) Okamoto, N.; Oguni, M. *Solid State Commun.* **1996**, *99*, 53. Okamoto, N.; Oguni, M.; Sagawa, Y. *J. Phys.: Condens. Matter* **1997**, *9*, 9187.